Energy Transfer and Activated Chemiluminescence during Thermal Oxidation of Polypropylene: Evidence for Chemically Induced Electron Exchange Luminescence

Idriss Blakey,[†] Graeme A. George,*[,†] and Norman C. Billingham[‡]

Centre for Instrumental and Developmental Chemistry, Faculty of Science, Queensland University of Technology, Brisbane, Queensland, Australia, 4001; and School of Chemistry, Physics and Environmental Sciences, The University of Sussex, Falmer, Brighton, BN1 9QJ, U.K.

Received February 5, 2001; Revised Manuscript Received August 21, 2001

ABSTRACT: The mechanism of chemiluminescence (CL) during thermal oxidation of polypropylene (PP) was probed by doping PP with an energy acceptor (9,10-dibromoanthracene [DBA]) and a chemiluminescence (CL) activator (9,10-diphenylanthracene [DPA]). Doping PP with DBA had little effect on the shape of the CL intensity (I_{CL})−time profile. This suggests that energy transfer from triplet states is probably not significant in the scheme of PP CL. However, the CL activator (DPA) had a significant effect on the shape and intensity of the I_{CL}−time profile. In the absence of DPA, the I_{CL}−time profile matches the profile for the formation of carbonyl-containing oxidation products from FTIR-emission spectra. In contrast, in the presence of DPA, it was the *integrated* DPA I_{CL}−time profile which matched the oxidation product profile, indicating that now I_{CL} was proportional to the hydroperoxide concentration. It is suggested that peroxides formed during PP oxidation are capable of reacting with DPA to produce chemically induced electron exchange luminescence (CIEEL). It is also suggested that CL from undoped PP, i.e., direct CL, may also occur by a CIEEL mechanism. This mechanism is believed to involve the reaction of PP peroxides with an easily oxidizable luminescent oxidation product. For the detector system used in this study the majority of light emitted is consistent with reactions between acyl peroxides and α,β-unsaturated carbonyls. The consequences of this mechanism are that the I_{CL}−time curve measured during the oxidation of PP may reflect either the hydroperoxide profile or the oxidation product profile depending on the spectral wavelength analyzed or the state of purity of the polymer.

Introduction

Three processes can yield electronically excited states during chemical reactions, which then lead to the emission of visible light or chemiluminescence (CL). As shown in Scheme 1, these are direct, indirect, and activated CL.[1] The emission of CL from polymers has been most studied during the oxidation of the solid polymer and it has generally been regarded to be from a particular elementary reaction in the free radical oxidation sequence.

Direct Chemiluminescence (CL). Direct CL involves formation of excited states directly from chemical reactions and then light emission during relaxation of those excited states to the ground state (see eq 1). An example of a direct CL reaction is dioxetane decomposition.[2] Dioxetanes decompose directly to form excited carbonyls in the triplet or singlet state. However, the precise mechanism regarding the excitation step has been a matter of contention.[2−5]

Indirect CL. Often the initial electronically excited state formed in a direct CL reaction is nonluminescent or has low luminescence efficiency.[1] Under such circumstances, it is often useful to enhance the light intensity by adding energy transfer agents, such as 9,10-dibromoanthracene or biacetyl, to the system.[1] In this situation, energy transfer between an energy acceptor and the original excited molecule occurs, forming an excited energy acceptor. Light emission then occurs during relaxation of the energy acceptor to the ground state. This process is termed indirect CL and is represented generically in eq 2. The decomposition of secondary esters in solution is an example of a system where increased emission occurs on adding energy transfer agents. Dixon et al.[1] observed that light emission during the decomposition of secondary peresters was extremely weak and found that addition of DBA or biacetyl intensified light emission.

Scheme 1

Direct Chemiluminescence (e.g. Dioxetanes)

$$R \longrightarrow P^* \longrightarrow P + h\nu \qquad (1)$$

Indirect Chemiluminescence (e.g. Peresters + DBA)

$$R \longrightarrow P^* \xrightarrow{F} P + F^* \longrightarrow F + h\nu \qquad (2)$$

Activated Chemilumiescence (e.g. CIEEL)

$$R + A \longrightarrow R\cdot\cdot A \longrightarrow P + A^* \qquad (3)$$

$$A^* \longrightarrow A + h\nu$$

Activated CL. Activated CL involves emission of light from an excited state formed via a bimolecular reaction between a substrate and catalyst (see eq 3). An example of activated CL is light emission via a chemically initiated electron exchange luminescence[6] (CIEEL) mechanism. This type of mechanism involves donation of an electron from an activator to peroxide forming an activator radical cation and a peroxidic radical anion. The peroxidic radical anion rearranges and then undergoes electron exchange with the activator radical cation to form an excited activator. Typically, the CL activator is an easily oxidizable fluorescent polyaromatic hydro-

* To whom correspondence should be directed. E-mail: g.george@qut.edu.au.
[†] Queensland University of Technology.
[‡] The University of Sussex.

10.1021/ma010217t CCC: $20.00
Published on Web 11/22/2001

Scheme 2

Energy Transfer Mechanism

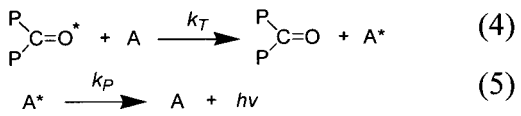

(4)

(5)

carbon, such as 9, 10-diphenylanthracene or rubrene.[7−10] The efficiency of the CIEEL reaction is related exponentially to the oxidation potential.

In addition, the peroxide needs to be able to be easily reduced.[2] Usually, the more easily the peroxide is reduced the more efficient the CIEEL mechanism. Hence, acyl peroxides usually yield highest efficiencies,[2] although simple hydroperoxides have also been shown to yield light via a CIEEL mechanism.[11]

The quantum yields of CIEEL reactions vary greatly depending on the system. For example, peroxyoxalate systems, which are believed to involve an intermolecular CIEEL mechanism, have been demonstrated to have quantum yields of up to 0.3 einstein mol^{-1}.[12] However, other systems such as the decomposition of diphenoyl peroxide have been shown to have quantum yields in the order of 2×10^{-5} einstein mol^{-1}.[13] Nonetheless, these values are several orders of magnitude higher than those estimated for CL from the reaction of a pair of peroxy radicals ($\sim 10^{-8}-10^{-10}$).[14]

CL from Oxidizing PP. For some time, chemical generation of excited states during thermal oxidation of polypropylene (PP) was considered to proceed via a direct CL mechanism involving the formation of triplet carbonyls, either via decomposition of a tetroxide formed via the Russell mechanism,[14−16] or via decomposition of hydroperoxides.[17−20] Both of these mechanisms predict that the I_{CL}−time profile should be proportional to the hydroperoxide concentration.[21,22] However, in a recent paper,[21] we demonstrated that PP I_{CL}−time profiles were proportional to the existing carbonyl concentration, which could not be explained in terms of these classical CL mechanisms. In light of this new evidence, two mechanisms were proposed. The first involves energy transfer, from an excited state formed via a classical mechanism, to a highly luminescent PP oxidation product (Scheme 2), i.e., indirect CL.

The kinetics of I_{CL}−time profiles that result from an energy transfer mechanism were predicted to be dependent on the concentration of the peroxidic species, [POOH], and the concentration of the luminescent oxidation product.[21] Equation 6 describes the kinetics of such a process, where k'_P is the rate constant for luminescence from A^*, k_d is the rate constant for hydroperoxide decomposition and ϕ_R, ϕ'_P and $\phi_{ET}(A)$ are the efficiencies for direct excitation, luminescence of the energy acceptor and energy transfer, respectively.

$$I_{CL} = k'_P [A^*] = \phi'_P \phi_{ET}(A) \phi_R k_d [POOH] \qquad (6)$$

For the production of carbonyl excited states, it is considered that the emitting species is a triplet state.

The second mechanism proposed involved the reaction of an acyl peroxide with an easily oxidizable luminescent oxidation product, via a CIEEL mechanism (Scheme 3). The kinetics of Scheme 3 are similar to Scheme 2, in that the rate of light emission, I_{CL}, is predicted to be dependent on the concentration of the peroxidic species and the concentration of the oxidation product (e.g., carbonyls) with CL activator properties, A. (eq 5).[21]

Scheme 3

Activated Chemiluminescence Mechanism

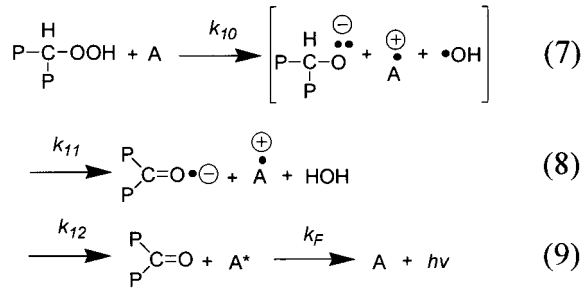

(7)

(8)

(9)

Equation 10 describes the kinetics of such a process, where k_{CIEEL} is the rate constant for the light reaction between peroxide and oxidation product with CL activator properties.

$$I_{CL} = k'_P [A^*] = \phi'_P \, k_{CIEEL} \, [POOH][A] \qquad (10)$$

Inspection of eqs 6 and 10 shows that in the absence of explicit knowledge of the concentration dependence of $\phi_{ET}(A)$ the two equations are kinetically equivalent; i.e., both are dependent on hydroperoxide and carbonyl concentration.

Kinetics and Mechanism of PP Oxidation. The two equations describing the intensity of CL, eqs 6 and 10, require information about the concentrations of the species present during oxidation, in particular the hydroperoxides and other oxidation products which may be luminescent. The oxidation of PP is known to be highly heterogeneous,[23−25] and oxidation−time profiles may be interpreted not as kinetic curves but rather reflecting the increasing fraction of the polymer that is oxidizing.[26] In one model for PP oxidation,[26,27] the oxidizing polymer is classified into three fractions. The first fraction consists of domains where no oxidation has taken place. The second consists of domains where the polymer is partially oxidized, i.e., has relatively high concentration of hydroperoxides and a relatively low concentration of carbonyls. The third fraction consists of domains where the polymer is highly oxidized, i.e. has relatively low concentrations of hydroperoxides and relatively high concentrations of carbonyls. In the highly oxidized region, there will be a higher proportion of acyl peroxides, due to further oxidation of oxidation products. Initially the model predicts a small proportion of domains that will be either "partially" or "highly" oxidized. During oxidation, small radicals generated in the partially oxidized regions diffuse into unoxidized regions to initiate oxidation converting them to partially oxidized regions. Therefore, this model predicts that there may be a physical separation of species. For example, a high proportion of hydroperoxides may be separated from the majority of carbonyl species. From such a model, the carbonyl curves can be interpreted as a statistical accumulation of highly oxidized domains.[28] Since the PP I_{CL}−time profile is proportional to the carbonyl−time profile, it can be concluded that a majority of light emission is occurring in the highly oxidized regions, where there is likely to be higher concentrations of acyl peroxides.

Differentiation of CL Mechanisms. A method to differentiate the energy transfer and CIEEL mechanisms is to monitor CL from PP doped with efficient energy acceptors and with CL activators. Since these will be randomly distributed throughout the polymer

as additives, they will be insensitive to the spatial distribution of polymer oxidation products described above. If an energy transfer mechanism is occurring, then the I_{CL}−time profile resulting from the added energy acceptor will be proportional to the concentration of peroxides, because the concentration of the added energy acceptor in eq 6 and thus $\phi_{ET}(A)$ will be constant.

Similarly, if a CIEEL mechanism is in operation, the I_{CL}−time profile for PP doped with a CL activator will be proportional to the peroxide concentration, because the concentration of the CL activator in eq 10 will be constant, provided the activator is not itself oxidized to a nonluminescent species.

This paper discusses the I_{CL}−time profiles obtained from oxidizing PP doped with an energy acceptor (9,-10-dibromoanthracene, DBA) and a CL activator (9,10-diphenylanthracene, DPA). Furthermore, these profiles are compared to carbonyl curves, which were obtained spectroscopically by FTIR emission.

Experimental Section

Materials: Unstabilized PP powder; Hostalen PPK0160 (Hoechst AG); melt flow index (MFI) at 230 °C of 2.16 kg at 0.9 g/min; crystallinity by XRD of 45%.[26] The powder was Soxhlet extracted with AR hexane for 6 h.

9,10-Diphenylanthracene, 9,10-dibromoanthracene, and HPLC grade heptane were obtained from Aldrich and used without further purification.

Doping of PP with DPA and DBA. DPA and DBA solutions at a concentration of 5×10^{-3} M were prepared in HPLC grade heptane. Doping of the powder was achieved by swelling the polymer in heptane solutions of DPA or DBA for 1 week in the dark. The powder was then filtered, washed with heptane, allowed to air-dry, and finally dried at a 760 mm vacuum for 24 h. A blank was prepared in a similar manner by swelling PP powder in HPLC grade heptane. To determine the concentration of DPA in the polymer, the sample was extracted with heptane and the concentration in the extract was determined using a calibration curve constructed from UV−Visible absorbance readings. The concentration of DPA in the polymer was determined to be 2×10^{-3} mol kg^{-1}.

Analysis of PP Samples Using the CL Apparatus. A single layer of PP particles (2.65 ± 0.01 mg) in an aluminum pan was used for analysis in the CL apparatus, which has been described elsewhere.[27,29] The polymer was heated to the oxidation temperature under an inert atmosphere of nitrogen and once the temperature had stabilized the gas was switched to pure oxygen. Photon counts integrated over a 10 s period were recorded continuously during oxidation. Oxidation of PP samples was performed at the following temperatures: 150, 140, 130, 120, and 100 °C.

Spectral Analysis of CL from Undoped PP. Using the sample presentation described above, relative contributions from different spectral regions were determined using a series of commercial sharp cutoff filters. The spectral ranges of the filters were determined using a Cary UV/vis spectrometer. To calculate the amount of light emitted from the 320−360 nm region, the I_{CL}−time profiles using a 360 nm cutoff filter were subtracted from the I_{CL}−time profile using a 320 nm cutoff filter. The I_{CL}−time profile for light from the 425−545 nm region was calculated by subtracting the I_{CL}−time profile using a 545 nm cutoff filter from the I_{CL}−time profile using a 425 nm cutoff filter.

Analysis of PP Doped with DPA Using CL-FTIR Infrared Emission. The simultaneous CL-FTIR emission spectrometer (CL-IES) has been described previously.[21,30,31] For FTIR emission spectroscopy, samples are required to be thin (<10 μm) and have intimate contact with the platinum hotplate to avoid formation of temperature gradients within the sample and absorption of the emitted light by the sample.[30,31] Therefore, individual particles of PP doped with DPA were pressed between polished steel disks in an hydraulic press (under 10 tons for 20 min) to form a thin film.

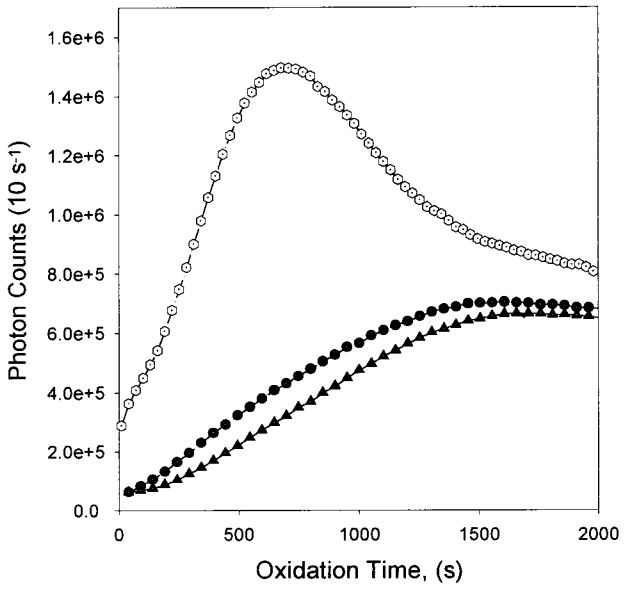

Figure 1. Comparison of I_{CL}−time curves for the oxidation at 150 °C of PP doped with DPA (−⬡−) and DBA (−●−) and undoped PP (−▲−). The sample analyzed was a thin layer of powder weighing 2.65 ± 0.01 mg.

The sample was heated to the oxidation temperature under an inert atmosphere of nitrogen, and when the temperature had stabilized the gas was switched to pure oxygen. FTIR emission spectra were averaged over 32 scans with a 4 cm^{-1} resolution (~25 s), and then the CL apparatus accumulated photon counts over a 35 s period. This sequence was repeated each minute during the oxidation of the polymer. Therefore, CL data and FTIR data could be obtained from an oxidizing single particle of PP almost simultaneously and in real time. For the runs where I_{CL} was of especially low intensity, the photon counts were averaged over longer time periods post analysis.

To convert the raw data from the FTIES to an emissivity spectrum, which is equivalent to an absorbance spectrum, a platinum background spectrum was subtracted and the result ratioed to a reference graphite spectrum.[30] A total carbonyl concentration−time profile was determined by plotting the area under the broad 1690−1780 cm^{-1}peak vs oxidation time.

Analysis of Undoped PP and PP Doped with DPA by CL-DSC. The simultaneous CL-DSC apparatus consisted of a Mettler Toledo DSC 821 differential scanning calorimeter that was modified at the University of Sussex to enable the attachment of a photomultiplier, the detector for the CL, above the sample. A thin layer of powder (2.85 ± 0.01 mg) was placed in an aluminum DSC pan for analysis. An empty aluminum DSC pan was used as a reference. The DSC pans were used uncapped to allow simultaneous monitoring of chemiluminescence intensity (I_{CL}) and heat flow. The photon counter in the CL apparatus was set to integrate over 10 s intervals. The DSC measured heat flow every second. The sample was heated to the oxidation temperature (150 °C) under a nitrogen atmosphere, and when the temperature had stabilized, the gas was switched to pure oxygen.

Results and Discussion

CL from PP Doped with Energy Acceptors and CL Activators. I_{CL}−time profiles for undoped PP and PP doped with DPA and DBA are shown in Figure 1. It is clear from the figure that doping PP with DPA has a large effect on the shape and intensity of the I_{CL}−time profile. The maximum intensity increases from approximately 600 000 to 1.6 million counts. Furthermore the position of the maximum shifts from about 1500 to

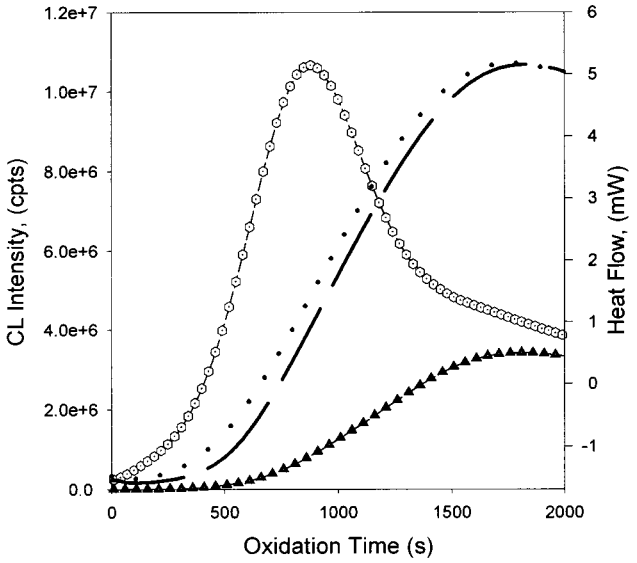

Figure 2. Comparison of DPA I_{CL}−time curve (−⬡−) with a PP I_{CL}−time curve (−▲−) and their respective DSC heat flow curves (• •, —) obtained from CL-DSC at 150 °C. The sample analyzed was a thin layer of powder weighing 2.85 ± 0.01 mg.

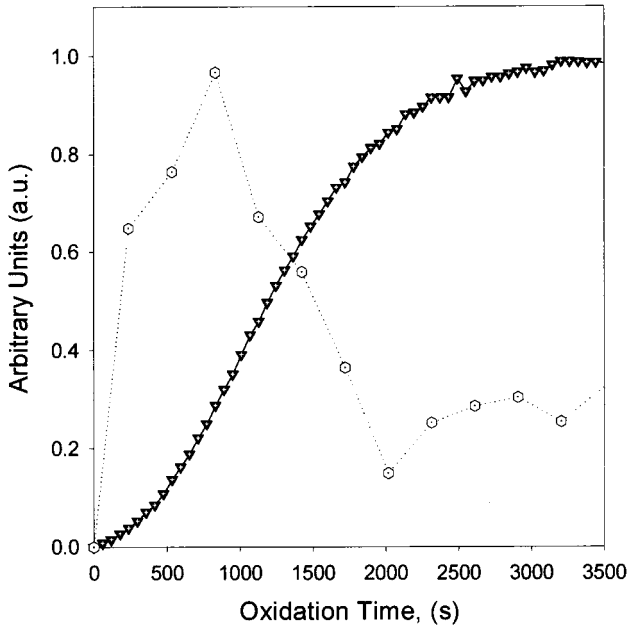

Figure 3. Comparison of the carbonyl curve (−▼−) and DPA I_{CL}−time curve (···⬡···) obtained from a single particle of PP using the CL-IES apparatus at 150 °C under an oxygen atmosphere.

approximately 750 s. In contrast, doping PP with DBA had only a minor effect on the I_{CL}−time profile. Similar results were obtained at 140, 130, 120, and 100 °C (results not shown). The possibility that DPA is significantly altering the PP autoxidation process can be ruled out from analysis of the results from CL-DSC and CL-IES respectively, which are described below.

CL-DSC of Undoped PP and PP Doped with DPA. Figure 2 compares the DSC heat-flow curves, obtained using the CL-DSC apparatus, of the thermal oxidation of undoped PP and PP doped with DPA. For a system where only one reaction is taking place, the heat flow, $\Delta Q_m/dt$, is related to the instantaneous rate of reaction.[32] However, DSC is a nonspecific technique, so for systems where there are multiple parallel reactions with different heats of reaction, ΔH_R, occurring simultaneously, a weighted average rate of reaction, ω, is obtained for any given point in time (eq 11).

$$\frac{\Delta Q_m}{dt} = \Delta H_{R1}\omega_1 + \Delta H_{R2}\omega_2 + \Delta H_{R3}\omega_3 + \cdots + \Delta H_{Rn}\omega_n \quad (11)$$

For auto-accelerating systems, such as oxidizing polymers, the heat flow curve will be sensitive to any additives that accelerate or slow the overall reaction, such as radical scavengers or hydroperoxide decomposers.[33] For the concentration of DPA used the differences in the heat-flow curves for PP doped with DPA and undoped PP are minimal and are typical of repeat runs for undoped PP. If DPA were accelerating the oxidation of PP, the heat-flow curves would show a corresponding change. However, there is no significant change despite the differences in the I_{CL}−time profiles for the two samples. It is therefore concluded that the DPA is altering the CL process and not the oxidation process of PP.

It should be noted that the time to maximum I_{CL} for the PP doped with DPA measured in the conventional CL apparatus and the CL-DSC apparatus are slightly different. This is due to the different reaction geometries of the two instruments. Oxidation reactions are very sensitive to factors such as the flow rate of oxygen, temperature, and headspace above sample. Usually, repeatability for a particular instrument will be good (± 1%), but when results between instruments are compared and the reaction conditions cannot be accurately reproduced then there will be differences, especially at higher temperatures where the rate of oxidation is higher. In addition, the different intensities observed for the DPA I_{CL}−time profiles in Figures 2 and 3 is due to the respective spectral sensitivities of the different CL apparatus used.

CL-IES of PP Doped with DPA. Previously,[21] we have demonstrated that I_{CL}−time profiles for oxidation of undoped PP at a range of temperatures were proportional to the corresponding carbonyl concentration−time curves, when analyzed using simultaneous CL-IES. Figure 3 compares the DPA I_{CL}−time profile and the carbonyl−time curve obtained from a simultaneous CL-IES experiment during thermal oxidation of PP doped with DPA. The carbonyl−time profile has a sigmoidal shape, which is typical of PP oxidation.[21] However, Figure 3 shows that the DPA I_{CL}−time profile is not proportional to the carbonyl curve, and interestingly, the maximum occurs at the inflection of the carbonyl curve, suggesting that it is the derivative of the carbonyl−time curve. This experiment also supports the earlier conclusion that DPA is not significantly accelerating the oxidation reaction because the shape of the carbonyl concentration time curve is unaffected by the presence of DPA.

Calculation of Corrected DBA and DPA I_{CL}— Time Profiles. Due to the low concentration of DPA and DBA in the polymer ($\sim 2 \times 10^{-3}$ mol kg^{-1}) the assumption can be made that DPA and DBA CL do not significantly affect the efficiency of the intrinsic PP CL. Furthermore, DPA is an inefficient triplet energy acceptor, compared to DBA and thus should not undergo a significant amount of energy transfer from the excited triplet state of carbonyls present in oxidizing PP. Therefore, I_{CL}−time profiles for DPA and DBA CL can

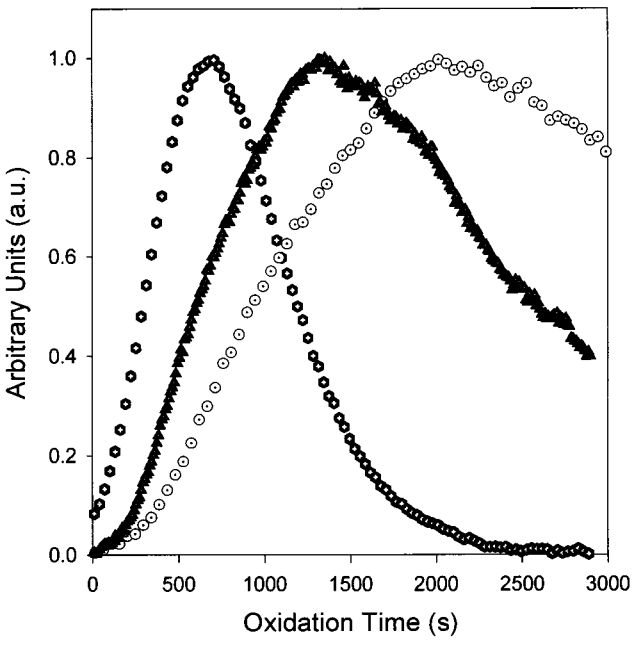

Figure 4. Comparison of normalized DPA (●), DBA (○), and PP (−▲−) I_{CL}−time profiles from the thermal oxidation of PP at 150 °C. The sample analyzed was a thin layer of powder weighing 2.65 ± 0.01 mg.

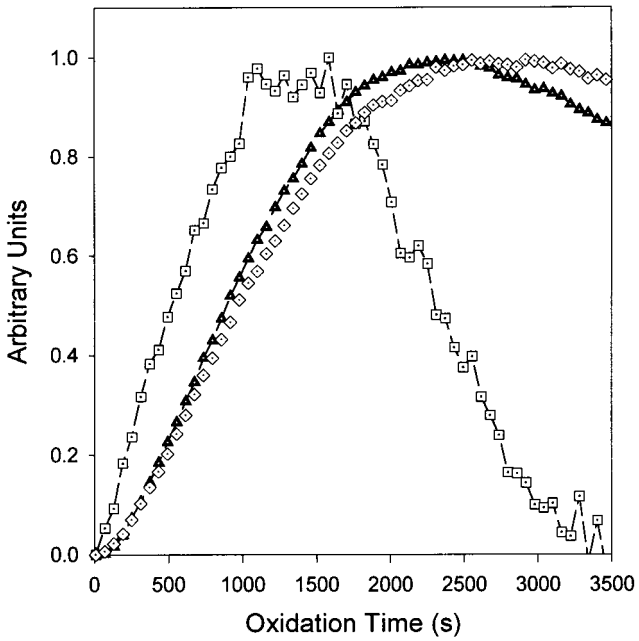

Figure 5. Comparison of the I_{CL}−time profile from the entire spectral range (−▲−) to I_{CL}−time profiles from 320 to 360 nm (−□−) and 425−545 nm (··◇··). Data were obtained from PP oxidizing at 150 °C under an oxygen atmosphere. The sample was analyzed as a thin layer of powder weighing 2.65 ± 0.01 mg.

be generated by subtracting the PP I_{CL}−time profile. The normalized PP and corrected DPA and DBA I_{CL}−time profiles for oxidation at 150 °C are shown in Figure 4. The rate of light emission from the DPA-doped sample rapidly increases to a maximum at 750 s and then decays relatively quickly compared to that from DBA-doped and undoped PP. The DBA curve rises to a maximum at approximately 1250 s and decays. The PP curve slowly rises to a maximum at about 2000 s and decays very slowly after the maximum. It is clear from this figure that each of these curves is different from the others. The DPA doped and undoped I_{CL}−time curves at 140, 130, 120, and 100 °C exhibited similar shapes to those observed Figure 4 except that the position of the I_{CL} maximum and the increased in an Arrhenius fashion and correspondingly the intensity at that maximum decreased according to an Arrhenius relationship (data not shown).

Explanation of DBA I_{CL}—Time Profile. The slight intensification of CL observed when DBA is added to PP in Figure 1 could be due to energy transfer from an excited carbonyl (e.g., produced through free radical recombination)[22] to the more luminescent DBA. In this case, energy transfer would involve an excited triplet carbonyl to singlet acceptor transition. Usually such a transition is highly spin forbidden and thus will have a low probability. However, for DBA the bromine substituents enhance the interaction between spin and orbital magnetic momenta (spin−orbit coupling) of electrons, which results in coupling of triplet and singlet states.[34−36] This increases the probability of triplet−singlet radiationless energy transfer compared to an unsubstituted anthracene. The higher fluorescence efficiency of DBA compared to the phosphorescence efficiency of triplet carbonyls results in intensification of the observed CL.

The first singlet-excited state of DBA is 3.04 eV above the ground state, which corresponds to a wavelength of 407 nm. Therefore, it would be expected that DBA would undergo triplet−singlet radiationless energy transfer from triplet-excited states of saturated carbonyls (e.g., saturated ketones emit phosphorescence at 360 nm, which is equivalent to a triplet state energy of 3.44 eV). Spectral analysis, described below, is consistent with this mechanism.

Spectral Distribution of PP CL. Analysis of the wavelength distribution of PP CL using a series of cutoff filters reveals that different wavelength regions have different I_{CL}−time profiles. For example, in Figure 5 two representative I_{CL}−time profiles, corresponding to light emitted in the ranges 320−360 and 465−545 nm respectively, are compared to the PP I_{CL}−time profile. Others,[37−39] have also observed light emission over such a broad range and have reported that the profiles from different wavelength regions are different. Furthermore, the phosphorescence maximum of thermo and photo-oxidized PP has been shown to shift to longer wavelengths with increasing oxidation times.[40,41] Typically, I_{CL}−time profiles for shorter wavelengths have a maximum earlier than the I_{CL}−time profiles of the longer wavelength light. This is precisely what we observe. The I_{CL}−time profile for the 320−360 nm region has a maximum at approximately 1500 s, which is earlier than the I_{CL}−time profile for the 425−545 nm region (2250 s). Radiation transmitted by the filter system from 320 to 360 nm will include the shoulder of triplet emission from saturated ketones having a peak at 390 nm,[37] while that transmitted by the filter system from 425 to 545 nm region will include emission from triplet unsaturated carbonyls.[42]

In Figure 6, it can be seen that the corrected DBA profile and the 320−360 nm I_{CL}−time profiles are similar. Hence, it appears that DBA is undergoing triplet−singlet energy transfer with triplet-excited carbonyls lying greater than 3.04 eV above ground state, as proposed in the earlier section.

Observation of an I_{CL}−time profile from the 360−320 nm region different from the PP I_{CL}−time profile necessitates analysis to determine whether classical

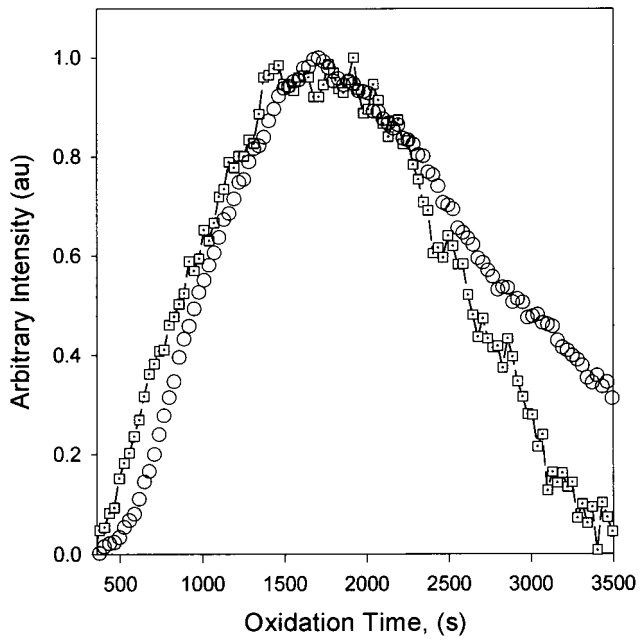

Figure 6. Comparison of the DBA I_{CL}−time curve (○) and the 320−360 nm region I_{CL} profile (−□−) for the thermal oxidation of PP at 150 °C.

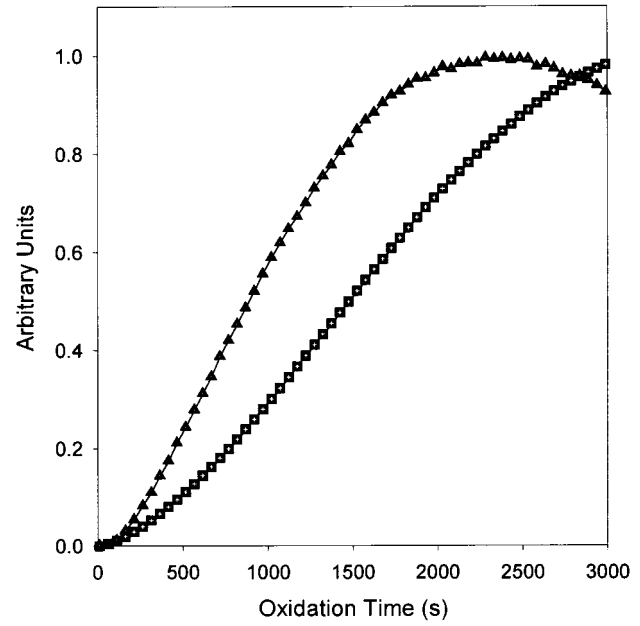

Figure 7. Comparison of the I_{CL}−time profile from the entire spectral region (−▲−) (which is equivalent to the carbonyl curve) to the integral of 320−360 nm I_{CL}−time profile from PP (−■−) oxidizing at 150 °C under an oxygen atmosphere.

mechanisms are responsible. Kinetic analysis of the Russell mechanism (peroxy radical termination) and that for CL from direct decomposition of hydroperoxides[21] have shown that I_{CL}−time profiles should be proportional to the hydroperoxide concentration, so that the integral of the I_{CL}−time profile should be proportional to the carbonyl−time curve. Hence, peroxy radical termination and direct decomposition of hydroperoxides can be tested as mechanisms for the production of CL from 320 to 360 nm by comparing the integral of the 320−360 nm region to carbonyl profile.[21] In Figure 7, it can be seen that the integral of the 320−360 nm region is not proportional to the I_{CL}−time profile from the entire spectral range. It should be noted that the I_{CL}−time profile from the entire spectral range is a good approximation of the shape for the carbonyl−time curve.[21] Therefore, classical mechanisms of CL cannot account for the 320−360 nm CL.

The 425−545 nm profile is almost identical to the PP I_{CL}−time profile with its maximum occurring at 2300 s, so clearly the integral of the curve will differ from the carbonyl profile. Hence, the 425−545 nm region also cannot be explained by classical mechanisms.

Explanation of DPA I_{CL}—Time Profile. The change in the PP I_{CL}−time profile when DPA is present cannot be due to energy transfer, because DPA and DBA have similar singlet energies (3.16 and 3.04 eV respectively). Furthermore, DBA should be a more efficient energy transfer agent for triplet−singlet transitions, due to enhanced spin−orbit coupling from the bromine functionalities. For example, Vassil'ev[34] observed that DBA was approximately 25 times more efficient than DPA at triplet−singlet energy transfer despite the higher fluorescence efficiency of DPA. If energy transfer were taking place, the DPA curve would be similar to the DBA profile. From the study of the CL-DSC of these samples, given earlier, it was ascertained that DPA is not accelerating the oxidation reaction, so some other explanation is required.

Further insight into the mechanism could be achieved by comparing data from the CL apparatus (PP and DPA I_{CL}−time curves) to the data from the CL-IES (PP I_{CL}−time and carbonyl concentration−time curves). However, comparison between experiments performed on an FTIES and a CL apparatus (as opposed to CL-IES) can be difficult, primarily because of the discrepancy in the sample size. For the CL experiments using the CL apparatus, sample sizes of 2.65 mg were used. This results in curves that are repeatable to ± 1%. However, infrared emission spectroscopy requires a small thin sample and, therefore, a flattened polymerization reactor particle was used (∼0.02 mg). It has been demonstrated that single particles can have inherently different stabilities due to varying amounts of residual stabilizer or polymerization catalyst.[29] This results in I_{CL}−time profiles being different for different particles, where all other experimental conditions are identical. These differences were determined to be due to sample heterogeneities such as differing amounts of residual stabilizer or polymerization catalyst. The consequence of this is that it is difficult to compare data from different instrumentation.

It has been demonstrated that the I_{CL}−time profiles from different particles collapse to a single master curve when the time scale is plotted on reduced coordinates ($t - t_{max}$, where t_{max} is the maximum of the I_{CL}−time profile).[45] In this study, we have sets of data from the CL apparatus, i.e. DPA and PP I_{CL}−time profiles and sets of data from the CL-IES, i.e., PP I_{CL}−time profiles and carbonyl concentration−time profiles. The respective sets have their own time scales because they have been collected under slightly different conditions. A common time scale can be calculated by ratioing the maxima of the PP I_{CL}−time profiles obtained in the CL apparatus and the CL-IES. When this was performed, PP I_{CL}−time curves from the CL apparatus and CL-IES overlay. Therefore, DPA I_{CL}−time profiles obtained with the CL apparatus can be plotted on the same time scale as the functional group profiles obtained by CL-IES. Hence, comparisons can be made between the data.

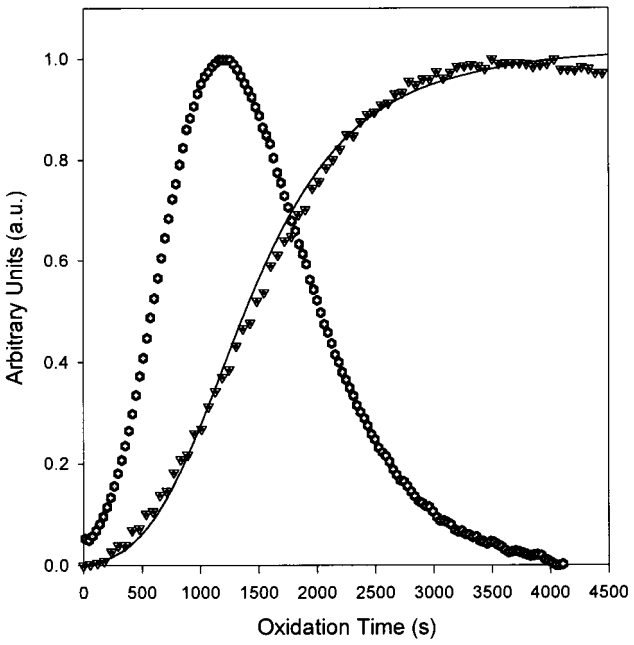

Figure 8. Comparison of a time normalized DPA I_{CL}−time profile (●) with the C═O (▽) profile obtained by FTIES during the oxidation of PP at 150 °C under an oxygen atmosphere. The solid line (—) represents the integral of the DPA I_{CL}−time profile.

Various authors[7−10,43,44] have demonstrated that DPA and other easily oxidizable polyaromatic hydrocarbons are capable of undergoing CIEEL reactions with various peroxides. Analysis of eq 6 indicates that if the CL activator concentration is constant, then the DPA I_{CL}−time profile will be proportional to the hydroperoxide concentration.

Previously,[21] we predicted that the integral of the hydroperoxide curve should be proportional to the carbonyl curve. This relationship is shown in eq 12, where ϕ_β is the fraction of alkoxy radicals, which undergo scission to produce carbonyls, and k_4 is the rate constant for the decomposition of hydroperoxides. Analysis of literature data for the oxidation of high impact polystyrene[46,47] and the PP[48] was consistent with the relationship in eq 12.

$$[\text{P═O}]_t = \phi_\beta k_4 \int_o^t [\text{POOH}]\, dt \qquad (12)$$

Therefore, if the corrected DPA I_{CL}−time profile is proportional to the hydroperoxide concentration, then the integral of this curve should be proportional to the carbonyl curve. In Figure 8, the normalized integral of the DPA I_{CL}−time profile is compared to the normalized carbonyl profile obtained by CL-IES. The integral of the DPA I_{CL}−time profile fits the carbonyl curve very well. This is a good result considering the data have been obtained from independent techniques. All these results are consistent with the DPA I_{CL}−time profile being proportional to the hydroperoxide concentration. Therefore, these results are also consistent with the hypothesis that DPA is reacting with peroxides formed during oxidation via a CIEEL mechanism.

In the introduction it was noted that the quantum yield of CIEEL reactions can range from 2×10^{-5} to as high as 0.3 einstein mol^{-1}.[12,13] These values are several orders of magnitude higher than those estimated for direct peroxide decomposition or radical termination reactions. From this it can be seen that only a small amount of CL activator is required to generate a significant amount of luminescence. In terms of the PP CL mechanism only a small amount of an easily oxidizable luminescent oxidation product needs to be formed via a side reaction to enable CL to be observed.

The fact that DBA does not react with peroxides to give a significant amount of luminescence can be easily explained in terms of a CIEEL mechanism. The oxidation potential of DBA is 1.42 eV, which is significantly higher than that of DPA, which is 1.20 eV.[7] The efficiency of CIEEL reactions is governed by the magnitude of the oxidation potential. In fact, the intensity of light emitted during a CIEEL reaction reduces exponentially with an increase in oxidation potential.[7−10,43,44] From extrapolation of the ln(light intensity) vs oxidation potential graph from *o*-xylylene peroxide[7] as an example, CIEEL light emission from DBA would be expected to be approximately 62 times less than that of DPA, when the greater fluorescence efficiency of DPA[49] is taken into account. The contribution to CL emission from a CIEEL mechanism will therefore be insignificant from DBA compared to DPA. It should be noted that this value would vary for different peroxides, the higher the reduction potential of the peroxide the lower the efficiency of the CIEEL reaction.

It has been suggested that consumption of DPA could be responsible for the drop in CL observed in Figures 1 and 2. In response to this, heating of DPA in pure oxygen at 150 °C yielded no observable light emission. Furthermore, a drop off in DPA luminescence was observed at the inflection point of the undoped I_{CL}−time profile for each oxidation temperature. A linear Arrhenius plot was obtained for the change in the position and intensity of the maximum of the DPA I_{CL}−time profile, which corresponded to the relationship obtained for undoped PP (data not shown). These results suggest that the DPA is not being converted into a nonluminescent species, but rather is merely acting as a catalyst, or is converted to a luminescent species with can also undergo CIEEL.

Further Analysis of DBA and 320—360 nm I_{CL}—Time Profile. Above it was established that the DPA I_{CL}−time profile is a good measure of the change in hydroperoxide concentration. Previously, we demonstrated that the direct PP I_{CL}−time profile is proportional to the carbonyl concentration measured by FT infrared emission spectroscopy.[21] Analysis of these curves can be performed to validate eq 10. Equation 10 predicts that if the CIEEL mechanism is operating, the PP I_{CL}−time profile will be proportional to the product of the hydroperoxide and CL activator concentration, where the CL activator is likely to be some carbonyl compound. Figure 9 shows a comparison of the corrected I_{CL} -time profile for PP containing DBA and the product of the I_{CL}−time profiles for PP with DPA (i.e., [ROOH]) and for PP free of additives (i.e., [C═O]). The curves show a good fit up to the maxima. The DBA I_{CL}−time profile represents the rate of emission of excited states with energies higher than 3.04 eV above the ground state and as shown earlier (Figure 7) is equivalent to the CL from undoped PP in the spectral range 320−360 nm. Therefore, it can be concluded that alkyl hydroperoxides reacting with some carbonyl compound is responsible for shorter wavelength CL. The kinetics of this reaction are consistent with those in eq 10 for a

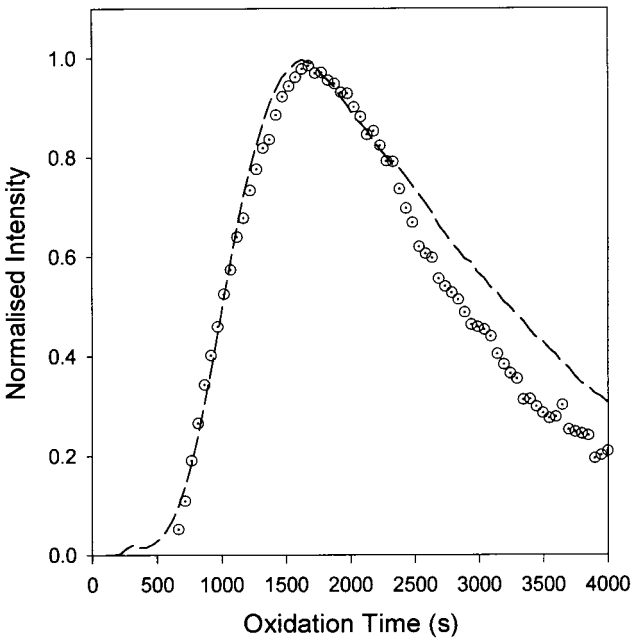

Figure 9. Comparison of DBA I_{CL}−time curve (○) and the product of the DPA I_{CL} (POOH) profile and the PP I_{CL}−time (C═O) profile (— —).

CIEEL reaction between a hydroperoxide and a carbonyl as the activator, A. Interpreting their CL experiments in terms of heterogeneous oxidation, Tiemblo et al.[39] concluded that lower wavelengths of PP CL are due to light emission in the oxidation front between the highly oxidized and unoxidized polymer, i.e., the partially oxidized region discussed in the Introduction in the framework of the heterogeneous model. In this region of the polymer, the concentration of alkyl hydroperoxides will be the highest.

Explanation of CL from the 425—545 nm Region. Longer wavelength emissions are consistent with luminescence from α,β-unsaturated ketones.[37,38,42] The CL from longer wavelength regions is proportional to the carbonyl concentration, or in heterogeneous terms is proportional to the number of highly oxidized domains. Tiemblo et al.[39] have also proposed that light emission from this wavelength region arises from reactions occurring in highly oxidized regions of the polymer. In these highly oxidized regions of the polymer, there will be higher concentrations of acyl peroxides due to oxidation of aldehydes. We propose that CL from longer wavelengths is due to a CIEEL reaction between acyl peroxides and α,β-unsaturated carbonyls as the activator, A. The extended conjugation of the α,β-unsaturated carbonyl will favor stabilization of the radical cation, so increasing the likelihood of CIEEL emission. Billingham et al.[15] have also proposed that a majority of CL observed during PP oxidation is from reactions involving acyl peroxides.

Therefore, CL from short and long wavelengths can be explained in terms of a CIEEL reaction between PP peroxides and easily oxidizable luminescent oxidation products. This situation is analogous to chemiluminescent decomposition of *o*-xylylene peroxide. Smith et al.[7,8] have shown that a luminescent decomposition product reacts with *o*-xylylene peroxide via a CIEEL mechanism to yield CL.

Some Implications of This Work. It is clear from this study that doping PP with a small amount of CL activator can have a significant effect on the shape of the I_{CL}−time profile. Therefore, one should be mindful of analyzing polymers containing additives, such as antioxidants, that may have CL activator properties. In many studies of CL from PP it has been reported that the integral of the I_{CL}−time curve is equivalent to the oxygen uptake curve.[16] This is consistent with the results here for activated CL and indicates the presence of easily oxidized (aromatic) hydrocarbon impurities in many polymers.

In earlier studies of the heterogeneous model for the oxidation of PP, I_{CL}−time curves have been used to determine parameters to model the spreading of PP oxidation.[26,50] In those studies, the PP I_{CL}−time profile was taken to represent the infectious fraction, which will be equivalent to the hydroperoxide or radical concentration. These studies indicate that this is not correct. Therefore, further analysis is required to model the oxidation data using DPA I_{CL}−time profiles, which will be a good measure of the infectious fraction.

Furthermore, the composition of the polymer itself may be important in the interpretation of I_{CL}−time curves as representing the oxidation curve for subsequent kinetic analysis. The thermal oxidation of polyamides is a prime example of this. Lánská et al.[51,52] demonstrated that polyamide (PA) samples with different amounts of carboxylic acid, methyl, or amine functionalities had significantly different I_{CL}−time curves. From this they concluded that CL could not be used to assess polyamide oxidative stability.[51] However, an analysis of their results in the light of the above conclusions enables the PA I_{CL}−time profiles to be better categorized into two shape types. These are the sigmoidal type, similar to PP I_{CL}−time profiles and the Gaussian type, similar to DPA I_{CL}−time profiles for PP. The sigmoidal shaped curves were related to the total oxygen uptake curves, while the Gaussian type curves were related to the derivative of the total oxygen uptake curves. Total oxygen uptake curves are a measure of the total amount of oxidation that has occurred and hence are similar to carbonyl profiles. It was found that PA samples with Gaussian type profiles had high amine concentrations. Amines have been demonstrated to react with various peroxides via a CIEEL type mechanism.[53−55] Hence, it can be concluded that amines are reacting with the PA hydroperoxides via a CIEEL mechanism to give a Gaussian type I_{CL}−time profile that will be a measure of the hydroperoxide concentration, or more correctly the rate of hydroperoxide decomposition. The sigmoidal curve could be due to the reaction of aldehydes formed during oxidation with hydroperoxides as proposed by Lánská et al.[51,52,56] Using this analysis, the Gaussian curves seen from polyamides can be treated as rate of oxidation curves and the sigmoidal curves as accumulation of oxidation to assess the stability of PA toward thermal oxidation. When analyzed in this way, the I_{CL}−time profiles have great usefulness in the assessment of polyamide oxidative stability.

Conclusions

CL emitted during the oxidation of PP was probed by the addition of fluorescent polyaromatic hydrocarbons, DBA and DPA. DBA was found to have little effect on PP CL. Therefore, energy transfer can be ruled out as a mechanism to explain the observed deviations that PP I_{CL}−time profiles show from that expected from classical CL mechanisms. DPA was found to have a significant effect on the PP I_{CL}−time profiles. CL-IES

and DSC−CL experiments demonstrated that the concentration of DPA used was not significantly affecting the rate of auto-acceleration. The corrected DPA I_{CL}−time profiles were found to be proportional to the hydroperoxide concentration. The DPA I_{CL}−time profile is consistent with a CIEEL reaction between DPA and polymer hydroperoxides.

Spectral analysis of the PP I_{CL}−time profiles showed that there are at least two different contributions from different wavelength regions: the first is from shorter wavelengths due to emission from saturated carbonyls and the second is from longer wavelengths due to α,β-unsaturated carbonyls. Analysis of the kinetics demonstrated that the shorter wavelength region, which is similar to the DBA I_{CL}−time profile, is consistent with the reaction of hydroperoxides with a carbonyl species via a CIEEL mechanism. The longer wavelength I_{CL}−time profile is proportional to the carbonyl concentration. Therefore, this light emission must be due to reactions occurring in the highly oxidized regions of the polymer. These reactions would most likely involve acyl peroxides and unsaturated carbonyls and could occur via CIEEL mechanism, which is a general mechanism for CL from peroxides.

Acknowledgment. The financial support of the Australian Research Council (Grant A29803983) and the Centre for Instrumental and Developmental Chemistry are greatly appreciated.

References and Notes

(1) Dixon, B. G.; Schuster, G. B. *J. Am. Chem. Soc.* **1979**, *101*, 3116−3118.
(2) Horn, K. A.; Koo, J.-y.; Schmidt, S. P.; Schuster, G. B. *Mol. Photochem.* **1978—1979**, *9*, 1−37.
(3) O'Neal, H. E.; Richardson, W. H. *J. Am. Chem. Soc.* **1970**, *92*, 6553−6557.
(4) Adam, A.; Baader, W. J. *J. Am. Chem. Soc.* **1985**, *107*, 410−416.
(5) Zaklika, K. A.; Thayer, A. L.; Schaap, A. P. *J. Am. Chem. Soc.* **1978**, *100*, 4916−4918.
(6) Schuster, G. B. *Acc. Chem. Res.* **1979**, *12*, 366−373.
(7) Smith, J. P.; Schrock, A. K.; Schuster, G. B. *J. Am. Chem. Soc.* **1982**, *104*, 1041−1047.
(8) Smith, J. P.; Schuster, G. B. *J. Am. Chem. Soc.* **1978**, *100*, 2564−2566.
(9) Koo, J.-y.; Schuster, G. B. *J. Am. Chem. Soc.* **1978**, *100*, 4496−4503.
(10) Koo, J.-y.; Schuster, G. B. *J. Am. Chem. Soc.* **1977**, *99*, 6107−6109.
(11) Van Gompel, J.; Schuster, G. B. *J. Org. Chem.* **1987**, *52*, 1465−1468.
(12) Catherall, C. L. R.; Palmer, T. F.; Cundall, R. B. *J. Biolumin. Chemilumin.* **1989**, *3*, 147−154.
(13) Catalani, L. H.; Wilson, T. *J. Am. Chem. Soc.* **1989**, *111*, 2633−2639.
(14) Kellogg, R. E. *J. Am. Chem. Soc.* **1969**, *91*, 5433−5466.
(15) Billingham, N. C.; Then, E. T. H.; Gijsman, P. *Polym. Deg. Stab.* **1991**, *34*, 263−277.
(16) George, G. A. In *Developments in Polymer Degradation−3*, 1st ed.; Grassie, N., Ed.; Applied Science Publishers: London, 1981.
(17) Reich, L.; Stivala, S. S. *Makromol. Chem.* **1967**, *105*, 74−82.
(18) Rychlý, J.; Matisová-Rychlá, L.; Jurcák, D. *Polym. Deg. Stab.* **2000**, *68*, 239−246.
(19) Matisová-Rychlá, L.; Rychlý, J. *Polym. Deg. Stab.* **2000**, *67*, 515−534.
(20) Achimsky, L.; Audouin, L.; Verdu, J.; Rychla, L.; Rychly, J. *Eur. Polym. J.* **1999**, *35*, 557−563.
(21) Blakey, I.; George, G. A. *Macromolecules* **2001**, *34*, 1873−1880.
(22) Vassil'ev, R. F. *Opt. Spectrosc. (Transl. Opt. Spektrosk.* **1964**, *18*, 131−135.
(23) Richters, P. *Macromolecules* **1970**, *3*, 262−265.
(24) Blakey, I.; George, G. A. *Polym. Deg. Stab.* **2000**, *70*, 269−275.
(25) Knight, J. B.; Calvert, P. D.; Billingham, N. C. *Polymer* **1985**, *26*, 1713.
(26) George, G. A.; Celina, M.; Lerf, C.; Cash, G.; Weddell, D. *Macromol. Symp.* **1997**, *115*, 69−92.
(27) Celina, M.; George, G. A. *Polym. Deg. Stab.* **1995**, *50*, 89−99.
(28) Celina, M.; George, G. A. *Polym. Deg. Stab.* **1993**, *42*, 323−335.
(29) Celina, M.; George, G. A.; Billingham, N. C. *Polym. Deg. Stab.* **1993**, *42*, 335−344.
(30) George, G. A.; Celina, M.; Vassallo, A. M.; Cole-Clarke, P. A. *Polym. Deg. Stab.* **1995**, *48*, 199−210.
(31) George, G. A.; Vassallo, A. M.; Cole-Clarke, P. A.; Celina, M. *Angew. Makromol. Chem.* **1995**, *232*, 105−118.
(32) Höhne, G. W. H.; Hemminger, W.; Flammershein, H.-J. *Differential Scanning Calorimetry an Introduction for Practitioners*, 1st ed.; Springer: Berlin, 1996.
(33) Billingham, N. C.; Bott, D. C.; Manke, A. S. In *Developments in Polymer Degradation−3*; Grassie, N., Ed.; Applied Science Publishers: London, 1981.
(34) Vassil'ev, R. F. *Nature* **1962**, *196*, 668−669.
(35) Vassil'ev, R. F. *Prog. React. Kinet.* **1967**, *4*, 305−353.
(36) Birks, J. B. *Photophysics of Aromatic Molecules*, 1st ed.; Wiley-Interscience: London, 1970.
(37) Lacey, D. J.; Dudler, V. *Polym. Deg. Stab.* **1996**, *51*, 109−113.
(38) Osawa, Z.; Wu, S.; Konoma, F. *Polym. Deg. Stab.* **1988**, *22*, 97−107.
(39) Tiemblo, P.; Gomez-Elvira, J. M.; Teyssedre, G.; Massines, F.; Laurent, C. *Polym. Deg. Stab.* **1999**, *65*, 113−122.
(40) Allen, N. S.; McKellar, J. F.; Phillips, G. O.; Wood, D. G. M. *J. Polym. Sci.* **1974**, *12*, 2647−2650.
(41) Allen, N. S.; McKellar, J. F.; Phillips, G. O. *J. Polym. Sci., Polym. Lett. Ed.* **1974**, *12*, 253−255.
(42) Marsh, G.; Kearns, D. R.; Schaffner, K. *J. Am. Chem. Soc.* **1971**, *93*, 3129−3137.
(43) Adam, W.; Cueto, O.; Yany, F. *J. Am. Chem. Soc.* **1978**, *100*, 2587−2589.
(44) Adam, W.; Cueto, O. *J. Am. Chem. Soc.* **1979**, *101*, 6511−6515.
(45) Celina, M.; George, G. A. *Polym. Deg. Stab.* **1993**, *40*, 323−335.
(46) Ghaffar, A.; Scott, A.; Scott, G. *Eur. Polym. J.* **1976**, *12*, 615−620.
(47) Scott, G. In *Developments in Polymer Degradation−1*; Grassie, N., Ed.; Applied Science Publishers: London, 1977.
(48) Iring, M.; László-Hedvig, Z.; Tüdös, F.; Kelen, T. *Polym. Deg. Stab.* **1983**, *5*, 467−480.
(49) Sawaki, Y.; Ogata, Y. *J. Am. Chem. Soc.* **1977**, *99*, 5412−5416.
(50) Tiemblo, P.; Gomez-Elvira, J. M. *Polym. Deg. Stab.* **2000**, *67*, 49−56.
(51) Lánská, B.; Matisová-Rychlá, L.; Brozek, J.; Rychlý, J. *Polym. Deg. Stab.* **1999**, *66*, 433−444.
(52) Lánská, B.; Doskocilova, D.; Matisová-Rychlá, L.; Puffr, R.; Rychlý, J. *Polym. Deg. Stab.* **1999**, *63*, 469−480.
(53) Sakanishi, K.; Nugroho, M. B.; Kato, Y.; Yamazaki, N. *Tetrahedron Lett.* **1994**, *35*, 3559−3562.
(54) Stevani, C. V.; Baader, W. J. *J. Phys. Org. Chem.* **1997**, *10*, 593−599.
(55) Stevani, C. V.; Lima, D. F.; Toscano, V. G.; Baader, W. J. *J. Chem. Soc.-Perkin Trans. 2* **1996**, 989−995.
(56) Lánská, B.; Matisová-Rychlá, L.; Rychlý, J. *Polym. Deg. Stab.* **1998**, *61*, 119−127.

MA010217T